

# An Active Contour Model Guided by LBP Distributions

Michalis A. Savelonas<sup>1</sup>, Dimitris K. Iakovidis<sup>1</sup>,  
Dimitris E. Maroulis<sup>1</sup>, and Stavros A. Karkanis<sup>2</sup>

<sup>1</sup> Dept. of Informatics and Telecommunications, University of Athens,  
15784, Athens, Greece

`rtsimage@di.uoa.gr`

`http://rtsimage.di.uoa.gr`

<sup>2</sup> Dept. of Informatics and Computer Technology, Lamia Institute of Technology,

3<sup>rd</sup> Kilometer, Old National Road, 35100, Lamia, Greece

`sk@teilam.gr`

**Abstract.** The use of active contours for texture segmentation seems rather attractive in the recent research, indicating that such methodologies may provide more accurate results. In this paper, a novel model for texture segmentation is presented, combining advantages of the active contour approach with texture information acquired by the Local Binary Pattern (LBP) distribution. The proposed LBP scheme has been formulated in order to capture regional information extracted from distributions of LBP values, characterizing a neighborhood around each pixel, instead of using a single LBP value to characterize each pixel. The log-likelihood statistic is employed as a similarity measure between the LBP distributions, resulting to more detailed and accurate segmentation of texture images.

## 1 Introduction

The automatic segregation of textures within images is generally viewed as an essential first step in various vision applications, such as medical image analysis, industrial monitoring of product quality, content-based image retrieval and remote sensing.

Because of its wide applicability, texture segmentation has been the subject of intensive research in many recent studies [1-5]. However, no known approach is able to consistently and accurately segment textured images [6]. A commonly used strategy for texture segmentation is to extract texture features on a pixel-by-pixel basis and then use some technique to segment the image based on the extracted features and potentially, on some additional spatial constraints. Overall quality of texture segmentation is determined by the quality of both texture features and the segmentation technique.

Early image segmentation approaches have been utilizing boundary-based local filtering techniques such as edge detection operators, which require additional edge-linking operations in order to establish the connectivity of edge segments. This problem has been resolved by employing active contour models [7], which directly result in continuous curves. These models involve the deformation of initial contours towards the boundaries of the image regions to be segmented. A recent active contour model, named Active Contour Without Edges (ACWE) [8] has been gaining increasing

interest due to its advantages: 1) it is region-based, enabling the delineation of regions defined by smooth intensity changes, 2) its level set formulation provides adaptability to topological changes, and 3) it does not impose any significant initialization constraint [8]. However, in the scalar ACWE model the contour evolution depends on the image intensities rather than on the textural content of the image to be segmented. Consequently, the scalar ACWE model cannot discriminate regions of different textures that have equal average intensities.

Latest advances in active contour research focus on using feature vectors to guide contour evolution, as in the case of the extended ACWE model for vector-valued images, proposed by Chan et al [9]. Within a texture segmentation framework, such active contour models use feature vectors that encode the textural content of an image by means of features deriving from Gabor and wavelet transforms [5], [10-11].

The Local Binary Pattern (LBP) distribution, introduced by Ojala et al. [12], offers an alternative approach to spatial texture representation. Unlike the Gabor features, which are calculated from the weighted mean of pixel values over a small neighborhood, the LBP operator considers each pixel in the neighborhood separately, providing even more fine-grained information. In addition, the LBP texture features are invariant to any monotonic change in gray level intensities, resulting in a more robust representation of textures under varying illumination conditions. Comparative studies have demonstrated that the use of LBP distributions may result in higher classification accuracy than Gabor and wavelet features with a smaller computational overhead [12-14].

In this paper we introduce a novel active contour model for texture segmentation guided by LBP distributions. Based on the fact that texture is a local neighborhood property, we have considered using regional information extracted from distributions of LBP values characterizing a neighborhood around each pixel, instead of using a single LBP value to characterize each pixel. In accordance with [15], the similarity between the LBP distributions is estimated by means of the log-likelihood statistic. Moreover, time performance considerations led us to reduce the length of the LBP distributions by limiting the number of pixels participating in the estimation of the LBP values, provided that the resulting LBP operator maintains adequate discriminative capability.

The rest of this paper is organized in five sections. Section 2 briefly reviews the formulation of the LBP operator. The proposed active contour model is presented in Section 3. The results from its application on two-textured images are apposed in Section 4. Finally, in Section 5 the conclusions of this study are summarized.

## 2 The Local Binary Pattern Operator

We adopt the formulation of the LBP operator defined in [15]. Let  $T$  be a texture pattern defined in a local neighborhood of a grey-level texture image as the joint distribution of the gray levels of  $P$  ( $P > 1$ ) image pixels:

$$T = t(g_c, g_0, \dots, g_{P-1}) \quad (1)$$

where  $g_c$  is the grey-level of the central pixel of the local neighborhood and  $g_p$  ( $p = 0, \dots, P-1$ ) represents the gray-level of  $P$  equally spaced pixels arranged on a circle of radius  $R$  ( $R > 0$ ) that form a circularly symmetric neighbor set.

Much of the information in the original joint gray level distribution (1) about the textural characteristics is conveyed by the joint difference distribution:

$$T \approx t(g_0 - g_c, \dots, g_{P-1} - g_c) \tag{2}$$

This is a highly discriminative texture operator. It records the occurrences of various patterns in the neighborhood of each pixel in a  $P$ -dimensional vector.

The signed differences  $g_p - g_c$  are not affected by changes in mean luminance; resulting in a joint difference distribution that is invariant against gray-scale shifts. Moreover, invariance with respect to the scaling of the gray-levels is achieved by considering just the signs of the differences instead of their exact values:

$$T \approx t(s(g_0 - g_c), \dots, s(g_{P-1} - g_c)) \tag{3}$$

where

$$s(x) = \begin{cases} 1 & , x \geq 0 \\ 0 & , x < 0 \end{cases} \tag{4}$$

For each sign  $s(g_p - g_c)$  a binomial factor  $2^p$  is assigned. Finally, a unique  $LBP_{P,R}$  value that characterizes the spatial structure of the local image texture is estimated by:

$$LBP_{P,R} = \sum_{p=0}^{P-1} s(g_p - g_c) 2^p \tag{5}$$

The distribution of the  $LBP_{P,R}$  values estimated over an image region comprises a highly discriminative feature vector for texture segmentation [14-17].

### 3 Active Contour Model Guided by LBP Distributions

The proposed active contour model is inspired by the ACWE model for vector-valued images [9], which uses single point information to guide contour evolution. In what follows, we firstly review this original model and secondly we appose the formulation of the proposed model that uses regional information to guide contour evolution.

#### 3.1 The Original Model

The ACWE model for vector-valued images is based on Mumford-Shah functional [18] and the level set formulation [19]. This model was originally proposed for the segmentation of color images using vectors formed by the RGB values of the pixel intensities [9]. It was later adapted for texture segmentation using Gabor transform coefficients [11]. The model is formulated as follows:

Let  $u_0$  be the original image, defined on a planar domain  $\Omega$  with real values. Let  $u_0^i$ , for  $i=1, \dots, b$ , be the components that describe the original image  $u_0$ . Let  $C$  be the evolving contour. The two averages of  $u_0^i$  inside and outside the curve  $C$  are denoted as  $c_+^i$  and  $c_-^i$  for  $i=1, 2, \dots, b$ . Following [9], an energy functional  $E$  is introduced

which, when minimized with respect to  $\bar{c}_+ = (c_+^1, \dots, c_+^b)$ ,  $\bar{c}_- = (c_-^1, \dots, c_-^b)$ , and  $C$ , performs binary segmentation:

$$\begin{aligned}
 E(C, \bar{c}_+, \bar{c}_-) = & \mu \cdot \text{length}(C) + \\
 & \int_{\text{inside}(C)} \frac{1}{b} \sum_{i=1}^b \lambda_i^+ |u_0^i(x, y) - c_+^i|^2 dx dy + \\
 & \int_{\text{outside}(C)} \frac{1}{b} \sum_{i=1}^b \lambda_i^- |u_0^i(x, y) - c_-^i|^2 dx dy
 \end{aligned} \tag{6}$$

where each value  $u_0^i(x, y)$ ,  $i=1, \dots, b$ , is defined over a single point  $(x, y)$ . For example in [9],  $u_0^i(x, y)$  represents the RGB intensities at the point  $(x, y)$ , for  $i = 1, 2$ , and  $3$  respectively. The positive scalars  $\mu, \lambda_i^+$  and  $\lambda_i^-$  for  $i=1, \dots, b$ , are weight parameters for each image component. Minimizing the above energy, one tries to segment possible regions in the image with contours given by  $C$  and denoted as “inside  $C$ ”, from a uniform background denoted as “outside  $C$ ”.

In [9] the implementation has been done using the level set method of Osher and Sethian [19], which gives an efficient method for moving curves and surfaces, on a fixed regular grid, allowing for automatic topology changes, such as merging, breaking of curves etc.

The curve  $C$  is represented implicitly, via a level set function  $\phi(x, y)$  such that  $C = \{(x, y) : \phi(x, y) = 0\}$ , and  $\phi(x, y) > 0$  inside  $C$ ,  $\phi(x, y) < 0$  outside  $C$ . The energy  $E$  is expressed in level set formulation using the Heaviside function  $H$ , which is defined as:

$$H(x) = \begin{cases} 1 & , x \geq 0 \\ 0 & , x < 0 \end{cases} \tag{7}$$

and the Dirac Delta function  $\delta(x) = dH(x)/dx$ .

$$\begin{aligned}
 E(\bar{c}_+, \bar{c}_-, \phi) = & \mu \cdot \int_{\Omega} \delta(\phi(x, y)) |\nabla \phi(x, y)| dx dy + \\
 & \int_{\Omega} \frac{1}{b} \sum_{i=1}^b \lambda_i^+ |u_0^i(x, y) - c_+^i|^2 dx dy + \\
 & \int_{\Omega} \frac{1}{b} \sum_{i=1}^b \lambda_i^- |u_0^i(x, y) - c_-^i|^2 dx dy
 \end{aligned} \tag{8}$$

Minimizing  $E(C, \bar{c}_+, \bar{c}_-)$  with respect to the unknown constant vectors  $\bar{c}_+$ ,  $\bar{c}_-$  the following relations are obtained, embedded in a time-dependent scheme:

$$\begin{aligned}
 c_+^i(t) = & \frac{\int_{\Omega} u_0^i H(\phi) dx dy}{\int_{\Omega} H(\phi) dx dy}, \\
 c_-^i(t) = & \frac{\int_{\Omega} u_0^i (1 - H(\phi)) dx dy}{\int_{\Omega} (1 - H(\phi)) dx dy}
 \end{aligned} \tag{9}$$

i.e. the averages of component  $u_0^i$  inside and outside the curve  $C$  respectively, for  $i=1, 2, \dots, b$  where  $b$  is the number of components.

Minimizing  $E(C, \bar{c}_+, \bar{c}_-)$  with respect to  $\phi$ , and parameterizing the descent direction by an artificial time, the following Euler-Lagrange equation for  $\phi$  is obtained:

$$\frac{\partial \phi}{\partial t} = \delta(\phi) \left[ \mu \cdot \operatorname{div} \left( \frac{\nabla \phi}{|\nabla \phi|} \right) - \frac{1}{b} \cdot \sum_{i=1}^b \lambda_i^+ (u_0^i - c_i^+)^2 + \frac{1}{b} \cdot \sum_{i=1}^b \lambda_i^- (u_0^i - c_i^-)^2 \right] = 0 \quad (10)$$

where a smooth approximation of the Heaviside function  $H$  is used, as in [9].

Starting with an initial contour, given by  $\phi_0$ , at each time step the vector averages  $\bar{c}_+$ ,  $\bar{c}_-$  are updated and the partial differential equation in  $\phi$  is evolved. More details for the numerical aspects of the level set evolution can be found in [20].

### 3.2 The Proposed Model

The notion of texture is undefined at single pixel level and it is always associated with some set of pixels [21]. Moreover, as it is stated in Section 2, the single LBP values are texture pattern “signatures” and only their distribution over an image region provides a discriminative feature vector for texture segmentation. This motivated us to formulate the equations of the proposed model using the normalized histogram  $N^i(x, y)$ ,  $i=1, \dots, b$ , calculated considering regional LBP information, instead of using the single LBP values characterizing each pixel. This regional LBP information is captured by the distribution of the  $LBP_{P,R}$  values of all pixels that belong to a  $k \times k$  neighborhood centered at the pixel  $(x, y)$ . The  $i$ -th component, or “bin” of the normalized histogram  $N^i(x, y)$ ,  $i=1, \dots, b$  describes the probability of occurrence of a specific texture pattern on each  $k \times k$  neighborhood centered at a pixel  $(x, y)$  of the considered image region. The total number  $b$  of the histogram bins corresponds to the total number of the  $LBP_{P,R}$  values and is determined from the number of neighborhood pixels  $P$ . It should be noted that in previous vector active contour approaches, the value of each component  $u_0^i(x, y)$  of the vector  $u_0(x, y)$  is determined from a feature of the single point  $(x, y)$  and not from a region feature, as it is the case in the proposed model. For example, in [9]  $u_0^i(x, y)$  represents the RGB intensities at the point  $(x, y)$ , for  $i = 1, 2$ , and 3 respectively.

For the sake of efficiency, we choose  $LBP_{4,1}$  (Fig. 1) because it involves less complex computations than the standard  $LBP_{8,1}$  or other  $LBP_{P,R}$  ( $P > 8, R \geq 1$ ) operators and results in a shorter histogram of 16 bins. The  $LBP_{4,1}$  operator maintains adequate discriminative capability within the current segmentation framework, as demonstrated by our segmentation results. The use of vector quantization alternatives that have been commonly used instead [16], would introduce a significant computational overhead to the estimation of the feature vectors.

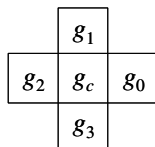


Fig. 1. Local neighborhood of pixels for  $LBP_{4,1}$

A rule of thumb suggests that the number of entries for each bin of a histogram should be at least 10. Considering that the  $LBP_{4,1}$  produces a 16-bin histogram, the number of entries required for the whole histogram is at least  $16 \times 10 = 160$ . Therefore  $k=13$  corresponds to the minimum neighborhood that satisfies this requirement ( $13^2=169 > 160$ ).

In [15], it is suggested that the similarity between the LBP histograms can be estimated by means of the log-likelihood statistic  $L$ . Within our context, the log-likelihood statistic  $L$  can be employed as a similarity measure between the LBP normalized histogram  $N(x, y)$  and the average LBP histograms  $\bar{c}_+$  and  $\bar{c}_-$  of the region inside and outside the contour respectively:

$$L(N, \bar{c}_+) = \sum_{i=1}^b N^i(x, y) \log c_+^i \quad \text{and} \quad L(N, \bar{c}_-) = \sum_{i=1}^b N^i(x, y) \log c_-^i \tag{11}$$

where  $N^i(x, y)$  is the  $i$ -th bin of the local LBP normalized histogram  $N(x, y)$ ,  $c_+^i$  ( $c_-^i$ ) is the  $i$ -th bin of the average LBP histogram  $\bar{c}_+$  ( $\bar{c}_-$ ), and  $b$  is the total number of histogram bins of the considered LBP probability distributions (equal to 16 for the operator  $LBP_{4,1}$ ). As  $L$  is an increasing function of similarity of the histograms  $N^i(x, y)$  and  $c_+^i$  ( $c_-^i$ ), we use  $(1-L)$  as a distance measure between the considered histograms, instead of their squared differences, suggested by equation (6) of the original model. Thus, (6) is replaced by:

$$E(C, \bar{c}_+, \bar{c}_-) = \mu \cdot \text{length}(C) + \int_{\text{inside}(C)} \frac{1}{b} \sum_{i=1}^b \lambda_i^+ (1 - N^i(x, y) \log(c_+^i)) dx dy + \int_{\text{outside}(C)} \frac{1}{b} \sum_{i=1}^b \lambda_i^- (1 - N^i(x, y) \log(c_-^i)) dx dy \tag{12}$$

Minimizing  $E(C, \bar{c}_+, \bar{c}_-)$ , results in a segmentation of regions characterized by a different average LBP probability distribution than the rest of the image. The positive scalars  $\lambda_i^+$  and  $\lambda_i^-$  for  $i=1, \dots, b$ , are weight parameters for the  $i$ -th bin of the LBP histograms  $N(x, y)$ ,  $\bar{c}_+$  and  $\bar{c}_-$ . Similarly to (6), the regions to be segmented are defined by contours given by  $C$  and denoted as “inside  $C$ ”, whereas the background region is denoted as “outside  $C$ ”.

The Euler-Langrange formulation of (12), which corresponds to equation (10) of the original model becomes:

$$\frac{\partial \phi}{\partial t} = \delta(\phi) \left[ \mu \cdot \text{div} \left( \frac{\nabla \phi}{|\nabla \phi|} \right) - \frac{1}{b} \cdot \sum_{i=1}^b \lambda_i^+ (1 - N^i(x, y) \log(c_+^i)) + \frac{1}{b} \cdot \sum_{i=1}^b \lambda_i^- (1 - N^i(x, y) \log(c_-^i)) \right] = 0 \tag{13}$$

where  $\phi$  is the level set function, implicitly representing curve  $C$ .

## 4 Results

The proposed active contour model is implemented and applied for the segmentation of two-texture images, composed of Brodatz textures [22], as well as of natural scenes obtained from VisTex database [23]. In order to evaluate the contribution of the log-likelihood statistic to segmentation accuracy, we perform experiments with: 1) the proposed model employing the log-likelihood statistic, as stated in equation (12), 2) the proposed model employing the squared differences of  $N^i(x, y)$  and  $c^i_+$  ( $c^i_-$ ), as suggested by equation (6) of the original model. Both variations of the proposed model are implemented in Microsoft Visual C++ and executed on a 3.2 GHz Intel Pentium IV workstation. The model constants are generally chosen as follows:  $\lambda^i_+ = \lambda^i_- = 750000$ ,  $\mu = 6500$  for the first variation, and  $\lambda^i_+ = \lambda^i_- = 750$ ,  $\mu = 6500$  for the second variation. These two sets of values were empirically determined to achieve higher segmentation accuracy in the majority of the two-texture images used. The LBP operator used is  $LBP_{4,1}$  and each local LBP histogram is extracted from  $k \times k$  neighborhoods with  $k=13$ , as described in the previous section.

Figures 1-4 illustrate four example results of the application of both variations of the proposed model on two-texture images. The results of the application of the first model variation, employing the log-likelihood statistic, are depicted on Fig. 1(a), 2(a), 3(a), 4(a) whereas the results of the second model variation, employing the squared differences of  $N^i(x, y)$  and  $c^i_+$  ( $c^i_-$ ), are depicted on Fig. 1(b), 2(b), 3(b), 4(b). The

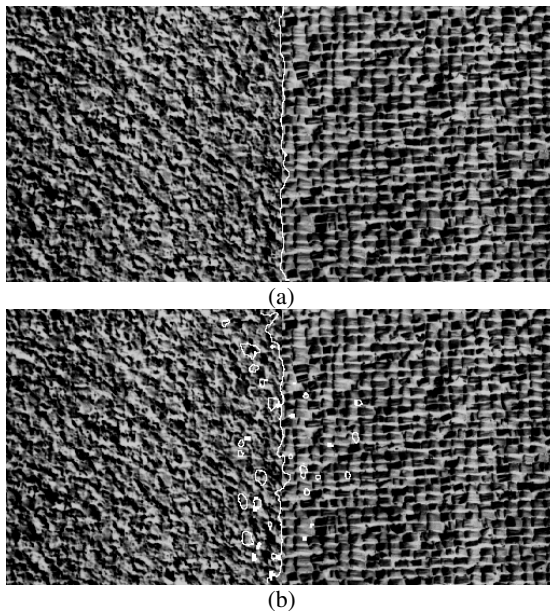


**Fig. 1.** Segmentation results of the application of the two model variations on the two-texture image D4D84, composed of Brodatz textures [22]: (a) segmentation result of the first model variation, (b) segmentation result of the second model variation

segmentation results obtained by the first model variation, employing the log-likelihood statistic, are very promising. The frames composed of different texture patterns are very well segmented. Moreover, the segmentation quality obtained by the application of the first model variation is generally improved when compared to that obtained by the second model variation, in the cases of Fig. 1,3,4 (in the case of Fig. 2, both variations achieved a practically perfect segmentation result). This improvement indicates that the log-likelihood statistic is more descriptive within the current segmentation framework. The computational cost of our approach varies between 40 and 60 seconds.

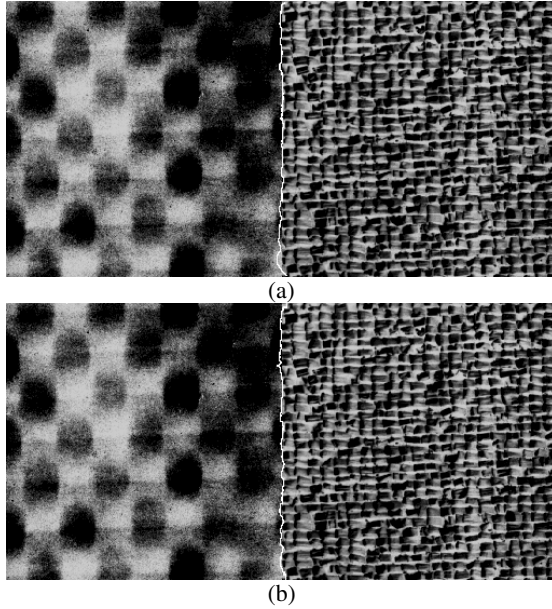


**Fig. 2.** Segmentation results of the application of the two model variations on the two-texture image D8D84, composed of Brodatz textures [22]: (a) segmentation result of the first model variation, (b) segmentation result of the second model variation

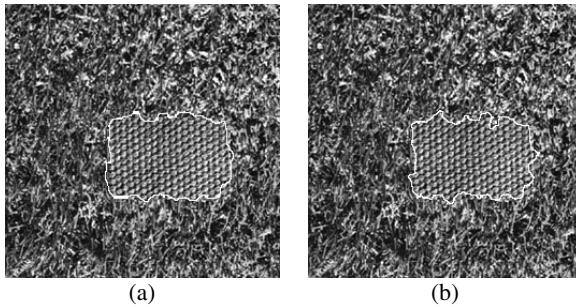


**Fig. 3.** Segmentation results of the application of the two model variations on the two-texture image D9D77, composed of Brodatz textures [22]. It should be noted that the “ground-truth” shape of the region to be segmented is a rectangular: (a) segmentation result of the first model variation, (b) segmentation result of the second model variation.

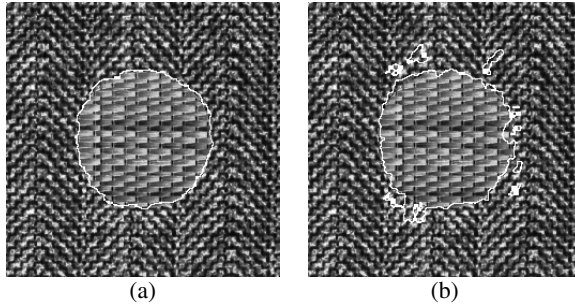


**Fig. 4.** Segmentation results of the application of the two model variations on the two-texture image D17D55, composed of Brodatz textures [22]: (a) segmentation result of the first model variation, (b) segmentation result of the second model variation

The results illustrated in Fig. 5 show that the proposed active contour model is able to achieve high quality segmentation of natural scenes.

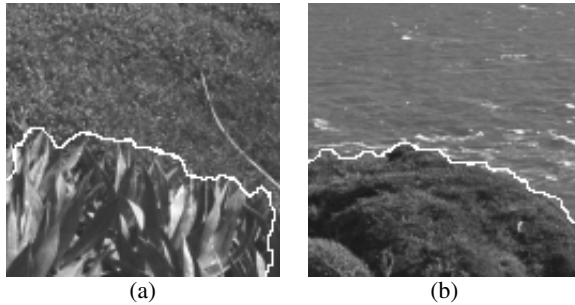


**Fig. 5.** Segmentation results of the application of the two model variations on natural scenes obtained from VisTex database [23]: (a) GrassPlantsSky.0005, (b) GroundWaterCity.0001

## 5 Conclusion

In this paper, we presented a novel model for texture segmentation, featuring an active contour approach. The proposed active contour model is guided by the texture information, which is encoded with the use of a local binary pattern scheme. The texture information is extracted from distributions of LBP values, characterizing a neighborhood around each pixel, instead of using a single LBP value to characterize each pixel. As a similarity measure between the LBP distributions, we have used the log-likelihood statistic. We demonstrated that the proposed model achieves high quality segmentation results by applying the model on composite texture images taken from the Brodatz album. Possible future extensions of this work include : 1) an extensive testing on medical images instead of the artificial ones used in this work, 2) the adoption of a quantitative measure for a more accurate evaluation of the segmentation results, 3) test the model performance when adopting the  $LBP_{p,R}^{riu2}$  operator introduced

in [15], and 4) extension of the proposed model for the segmentation of multiple-texture images by incorporating the multi-phase ACWE [24].

## Acknowledgement

This work was supported by the Greek General Secretariat of Research and Technology and the European Social Fund, through the PENED 2003 program (grant no. 03-ED-662).

## References

1. Theodoridis S., Koutroumbas K.: Pattern Recognition, 2<sup>nd</sup> edn., Academic Press (2003)
2. Mirmehdi M., Petrou M.: Segmentation of Color Textures, IEEE Transactions on Pattern Analysis and Machine Intelligence, Vol. 22, No. 2 (2000) 142-159
3. Quing X., Jie Y., Siyi D.: Texture Segmentation using LBP embedded Region Competition, Electronic Letters on Computer Vision and Image Analysis, Vol. 5, No.1 (2005) 41-47
4. Rousson M., Brox T., Deriche R.: Active Unsupervised Texture Segmentation on a Diffusion Based Feature Space, Proceedings of IEEE Conference on Computer Vision and Pattern Recognition, Madison, Wisconsin, USA (2003)
5. Sagiv C., Sochen N.A., Zeevi Y.: Integrated Active Contours for Texture Segmentation, IEEE Transactions on Image Processing, Vol. 1, No. 1 (2004) 1-19
6. Clausi D.A., Deng H.: Design-Based Texture Feature Fusion Using Gabor Filters and Co-Occurrence Probabilities, IEEE Transactions on Image Processing, Vol. 14, No. 7 (2005) 925-936
7. Kass M., Witkin A., Terzopoulos D.: Snakes: Active Contour Models, International Journal on Computer Vision, Vol. 1 (1988) 321-331
8. Chan T.F., Vese L.A.: Active Contours Without Edges, IEEE Transactions on Image Processing, Vol. 7 (2001) 266-277
9. Chan T., Sandberg B., Vese L., Active Contours Without Edges for Vector-Valued Images, Journal of Visual Communication and Image Representation, Vol. 11(2002) 130-141
10. Paragios N., Deriche R.: Geodesic Active Contours for Supervised Texture Segmentation, Proceedings of IEEE International Conference on Computer Vision and Pattern Recognition (1999) 2422-2427
11. Aujol J.F., Aubert G., Blanc-Feraud L.: Wavelet-Based Level Set Evolution for Classification of Textured Images, IEEE Transactions on Image Processing, Vol. 12, No. 12 (2003) 1634-1641
12. Ojala T., Pietikäinen M., Harwood D.: A Comparative Study of Texture Measures with Classification based on Feature Distributions, Pattern Recognition, Vol. 29 (1996) 51-59
13. Paclik P., Duin R., Kempen G.V., Kohlus R.: Supervised Segmentation of Textures in Backscatter Images, Proceedings of IEEE International Conference on Pattern Recognition, Vol. 2 (2002) 490-493
14. Mäenpää, T., Pietikäinen, M.: Classification with color and texture: Jointly or separately?, Pattern Recognition, 37 (8) (2004) 1629-1640
15. Ojala T., Pietikäinen M, Mäenpää T.: Multiresolution Gray-Scale and Rotation Invariant Texture Classification with Local Binary Patterns, IEEE Transactions on Pattern Analysis and Machine Intelligence, Vol. 24, No. 7, (2002) 971-987

16. Pietikäinen M., Ojala T., Nonparametric Texture Analysis with Simple Spatial Operators, Proceedings of 5<sup>th</sup> International Conference on Quality Control by Artificial Vision, Trois-Rivieres, Canada (1999) 11-16
17. Mäenpää T., Ojala T., Pietikäinen M., Maricor S.: Robust Texture Classification by Subsets of Local Binary Patterns, Proceedings of 15<sup>th</sup> International Conference on Pattern Recognition, Barcelona, Vol. 3 (2000) 947-950
18. Mumford D., Shah J.: Optimal Approximation by Piecewise Smooth Functions and Associated Variational Problems, Communications in Pure and Applied Mathematics, Vol. 42 (1989) 577-685
19. Osher S., Sethian J.: Fronts Propagating with Curvature- Dependent Speed: Algorithms Based on the Hamilton-Jacobi Formulations, Journal Of Computational Physics, Vol. 79, (1988) 12-49
20. Aubert G., Vese L.: A Variational Method in Image Recovery, SIAM Journal on Numerical Analysis, Vol. 34(5) (1997) 1948-1979
21. Unser, M. , Eden, M.: Nonlinear Operators for Improving Texture Segmentation Based on Features Extracted by Spatial Filtering. IEEE Trans. On Systems, Man and Cybernetics, 20 (4) (1990) 804-815
22. Brodatz P.: Textures: A Photographic Album for Artists and Designers, New York, NY, Dover (1996)
23. Vision Texture Database, MIT Media Lab, [www-white.media.mit.edu/vismod/imagery/VisionTexture/vistex.html](http://www-white.media.mit.edu/vismod/imagery/VisionTexture/vistex.html)
24. Vese L.A., Chan T.F.: A Multiphase Level Set Framework for Image Segmentation Using the Mumford and Shah Model, International Journal on Computer Vision, Vol. 50, No. 3 (2002) 271-293